American Journal of Civil Engineering
2013; 1(3): 111-123
Published online November 10, 2013 (http://www.sciencepublishinggroup.com/j/ajce)
doi: 10.11648/j.ajce.20130103.15

Evaluation of torsional capacity of square RC columns strengthened with CFRP using finite element modeling

Ahmed Sameer Younus[1, *], Ammar A. Abdul Rahman[2]

[1]Structural Engineering, Civil Engineering Department, Al Nahrain University, Baghdad, IRAQ
[2]Structural Engineering, Faculty Member, Civil Engineering Department, Al Nahrain University, Baghdad, IRAQ

Email address:
ahmedalkuhly@gmail.com(A. S. Younus), ammar.arahman@yahoo.com(A. A. A. Rahman)

To cite this article:
Ahmed Sameer Younus, Ammar A. Abdul Rahman. Evaluation of Torsional Capacity of Square RC Columns Strengthened with CFRP Using Finite Element Modeling. *American Journal of Civil Engineering.* Vol. 1, No. 3, 2013, pp. 111-123.
doi: 10.11648/j.ajce.20130103.15

Abstract: Researches on behavior of reinforced concrete (RC) columns subjected to torsion including mechanical properties like cracks and failure modes are not commonly studied and investigated well. It is necessary to investigate the mechanical properties and characteristics for RC columns subjected to torsion during different types of loading including earthquakes. Also, as a reinforcing method to existing RC structures, the application of Carbon Fiber Reinforced Polymers (CFRP) became common. CFRP has properties of high tensile strength, light weight and easy execution. CFRP is easy to adjust the reinforcement volume whenever necessary and considered excellent in endurance because the rust will not occur. The purpose of this study is to present a model suitable for analyzing square RC columns strengthened with CFRP under torsional effects and developing a reasonable method for calculating angles of twist for square concrete columns using the finite element method. Final available version of finite element analysis software [ANSYS 14 – 64 bits] is used to solve the problem and to predict the torsional behavior of the columns under investigation. The results are compared and verified with an experimental study and the numerical results showed acceptable agreement with the experimental results. Several important parameters affecting the torsional capacity of square columns strengthened with CFRP under torsion are studied in parametric study. These parameters include: the presence (distribution type) of CFRP, CFRP number of layers (thickness), type of interface between CFRP layers and concrete surface, CFRP orientation and effect of applying axial load in addition to torque. The results showed that zebra shape (where sheets are straight and fibers are inclined with 45^{o}) is the best way to increase the torsional capacity of RC columns.

Keywords: Torsion, RC Columns, CFRP, FEA, ANSYS

1. Introduction

As structures ages, many of them are reaching their design life. Others need strengthening to cope with increases in permitted loads due to the continuous revisions in applied codes of practice (e.g., truck axle loads and seismic loads). A lack of durability has also precipitated the need for repairs to many structural elements where steel reinforcement has corroded causing cracking then weakening of the bond, and sometimes even spilling of the concrete cover. One area where this is of concern is the repair and strengthening of columns as main structural elements in any structure. Severe corrosion of the reinforcing steel and the inconvenience of total replacement require that a nondestructive, easily applied method of protection and strengthening be used. These requirements are not restricted solely to the repair of old columns, however. Such a method can also be useful in other situations such as that which prompted these tests: the concrete test strength was less than the design strength for columns in a building under construction, and straight replacement of the columns was uneconomical and impractical [1].

Compression members, or columns are the key elements of all skeletal structures and may be defined as members carrying axial compressive loads, and whose length is considerably greater than the cross sectional dimensions. Such members may carry other types of loading, and may have end conditions and end moments of different kinds [2].

The inspections on typical reinforced concrete structures damaged during the past few earthquakes showed that some

columns in each of these structures were planned to joint beams to columns eccentrically. The concrete cracks, caused by the earthquakes, appeared spirally upwards round the surface of the columns, or developed obliquely along the whole length of the columns. These cracking patterns show that the column failure is a kind of torsional failure caused by the combination of torsion and shear [3].

Figure (1) shows some photos for concrete cracks appeared in number of Japanese buildings damaged in the past few earthquakes.

Photo. 1: Building damaged by the 1968 Tokachi-oki earthquake

Photo. 2: Building damaged by the 1978 Izu-Oshima earthquake

Photo. 3: Building damaged by the 1995 Hyogo-ken Nanbu earthquake

Photo. 4: Building damaged by 1997 Kagoshima-ken Hokuseibu earthquake

Photo. 5: Building damaged by 1997 Kagoshima-ken Hokuseibu earthquake

Figure (1). *Concrete cracks appeared in number of Japanese buildings damaged in the past few earthquakes [3]*

Research related to the strengthening of columns with Fiber Reinforced Polymers (FRP) composites is very limited; data or design guidelines are available in the literature only.

The lack of experimental and analytical studies along with the increasing interest in the use of FRP materials in the strengthening and rehabilitation of concrete columns that failed in torsion led to this study on torsional behavior of reinforced concrete columns strengthened with Carbon Fiber Reinforced Polymers (CFRP) laminates.

2. Finite Element Analysis

Since the problem under investigation has no exact (closed form) solution, numerical techniques have been adopted. The Finite Element Method (FEM) is nowadays one of the most frequently used computational method in solving scientific and engineering problems [4].

FEM analysis for members subjected to torsion is more difficult and complicated than that subjected to bending or shear. ANSYS 14 – 64bit was used to model, analyze and obtain results for specimens used in the verification study. The description of the ANSYS logical steps for modeling and results of analysis will be explained in the following subsections.

2.1. Geometry

All specimens of experimental study that adopted for verification have a square cross section of (200 mm x 200 mm) with length of (1300 mm). Normal concrete was casted with average compressive strength of (39.4 N/mm^2) and average tensile strength (3.24 N/mm^2). For Specimen (Re-1), longitudinal reinforcement was 4 D13 steel bars and transverse reinforcement was 7 D10 steel bars at intervals of 100 mm. Table (1) shows the material properties of reinforcing steel bars.

For Specimen (CFS-1), longitudinal reinforcement was 4 D13 steel bars and transverse reinforcement was CFRP at intervals of 100 mm. Four CFRP layers of 50 mm width were used for each piece where CFRP was arranged in one direction. The material properties of CFRP were shown in Table (2).

All specimens involved a central prestress bar of D19 in their reinforcement method with prestressing force of 200kN (5 N/mm^2). The geometry and reinforcing details of the specimens are shown in Figures (2) and (3) respectively.

Table (1). *Material Properties of Reinforcing Bars [5]*

Reinforcing Bar Type	Yield Strength (N/mm^2)	Tensile Strength (N/mm^2)	Young's Modulus (N/mm^2)
D10	360	515	2.06 x 10^5
D13	356	505	1.98 x 10^5

Table (2). *Material Properties of CFRP [5]*

Weight / Area ratio (g/m^2)	Thickness (mm)	Tensile Strength (N/mm^2)	Young's Modulus (N/mm^2)
600	0.333	3400	2.3 x 10^5

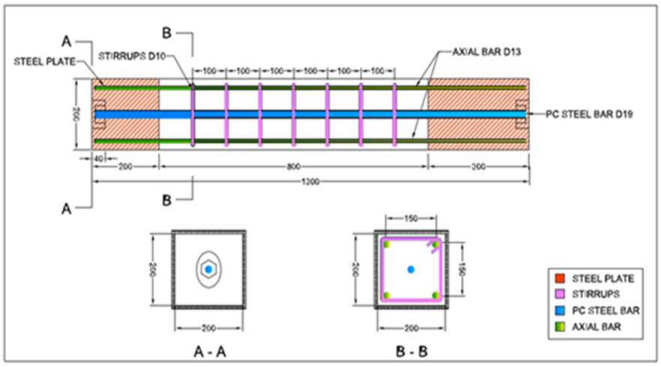

Figure (2). *Cross section in column specimen Re-1*

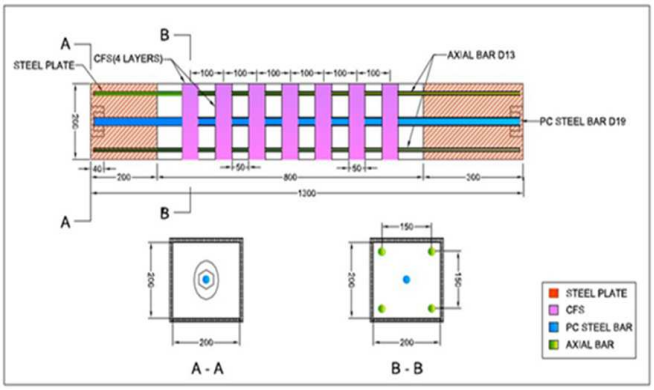

Figure (3.) *Cross section in column specimen CFS-1*

2.2. Elements Types

Using the ANSYS library of element types, the elements used in ANSYS modeling are shown in table (3).

Table (3). *Elements used in ANSYS modeling*

SPECIMENS	ELEMENT No.	ELEMENT TYPE	REPRESENTATION
Re-1	1	SOLID 65	Concrete
	2	LINK 8	Prestress Bar
	3	LINK 180	Longitudinal Reinf.
	4	LINK 180	Lateral Ties (Stirrups)
	6	SHELL 41	Steel Plate
CFS-1	1	SOLID 65	Concrete
	2	LINK 8	Prestress Bar
	5	SHELL 41	CFRP
	6	SHELL 41	Steel Plate

Table (4). *Real constants of elements used in ANSYS modeling*

REAL CONSTANT SET	ELEMENT TYPE	CONSTANT	VALUES
1	**SOLID65**	Material number	0
		Volume ratio	0
		Orientation angle	0
2	**LINK8**	Cross-sectional area (mm^2)	283.5
		Initial strain (mm/mm)	0.000027
3	**LINK180**	Cross-sectional area (mm^2) (Axial bars)	132.8
4	**LINK180**	Cross-sectional area (mm^2) (Ties)	78.6
5	**SHELL41**	Shell thickness at node I (mm)	1.33
		Shell thickness at node J (mm)	1.33
		Shell thickness at node K (mm)	1.33
		Shell thickness at node L (mm)	1.33
		Element x- axis rotation	90
		Elastic Foundation Stiffness (EFS)	0
		Added mass/unit area	0.0006
6	**SHELL41**	Shell thickness at node I (mm)	2
		Shell thickness at node J (mm)	2
		Shell thickness at node K (mm)	2
		Shell thickness at node L (mm)	2
		Element x- axis rotation	0
		Elastic Foundation Stiffness (EFS)	0
		Added mass/unit area	0.0006

2.3. Real Constants

Data which are required for the calculation of the element matrix, but which cannot be determined from the node locations or material properties are input as "real constants." Typical real constants include area, thickness, inner diameter, outer diameter, etc. A basic description of the real constants is given with each element type. The theory reference for the mechanical APDL and mechanical applications section describing each element type, shows how the real constants are used within the element. The real constants are input with the R command. The real constant values input on the command must correspond to the order indicated in the "Real Constants" list [6].

The real constant for SOLID65 element requires information about smeared reinforcement in three directions x, y and z (volume ratio, orientation angle, etc.). In this research discrete representation of steel reinforcement is

used, and smeared rebar is neglected, therefore all constants for SOLID65 element are equal to zero.

The real constant for LINK8 requires information about the cross sectional area of the reinforcing bar and its initial strain. It is no longer supported in GUI method in ANSYS 14 but can be used with command method just to represent the prestress bar constants.

The real constant for LINK180 requires information about the cross sectional area of the reinforcing bar.

The real constant for SHELL41 requires information about thickness of element in each node (the element may have variable thickness). In the present research, the element has a constant thickness; therefore the thickness values for all nodes are equal. Table (4) shows the real constants for all elements which are used in this work.

2.4. Materials Properties

The material properties for the two specimens used in this study are presented in detail as listed in Tables (5) and (6).

Material Model Number (1) refers to SOLID65 brick element. This element requires linear isotropic and multi-linear isotropic material properties to properly model the concrete. For linear isotropic, EX represents the modulus of elasticity of the concrete (E_c), and PRXY is Poisson's ratio of the concrete (ν_c). The modulus of elasticity of concrete is based on the ACI 318M-08 [7] equation.

$$E_c = 4700\sqrt{f_c'} \quad (1)$$

Poisson ratio for concrete is assumed to be 0.2 for all specimens based on the compressive strength of concrete used in all columns. The failure surface for compressive stresses is based on William and Warnke failure criterion [6] material model in finite element code ANSYS, version 14, the program requires that different constants to be defined, these constants are:-

1 Shear transfer coefficient for an open crack (f_{Jo}), C1.
2 Shear transfer coefficient for a closed crack (f_{Jc}), C2.
3 Uniaxial tensile cracking stress (f_{ct}, positive), C3.
4 Uniaxial crushing stress (f'_c, positive), C4.
5 Biaxial crushing stress (f'_{cb}, positive), C5.
6 Ambient hydrostatic stress state (σ_h) for use with constants 7 and 8, C6.
7 Biaxial crushing stress (f_1, positive) under the ambient hydrostatic stress state (constant 6), C7.
8 Uniaxial crushing stress (f_2, positive) under the ambient hydrostatic stress state (constant 6), C8.
9 Stiffness multiplier for cracked tensile condition, used if key option (7) is set to 1 for SOLID65 in finite element code ANSYS, version 14, (default to 0.6), C9.

Typical shear transfer coefficients range from 0.0 to 1.0, with 0.0 representing a smooth crack (complete loss of shear transfer) and 1.0 representing a rough crack (no loss of shear transfer). The shear transfer coefficients for open and closed cracks are determined using the work of Kachlakev et al. [8] as a basis: a convergence study is required when the shear transfer coefficient for the open crack drops below 0.2. The coefficient for open crack is set to 0.2, while the coefficient for closed crack is set to 0.7. The tensile strength of concrete used in this study is 3.24 MPa based on experimental study.

The biaxial crushing stress refers to ultimate biaxial compressive strength (f'_{cb}). The ambient hydrostatic stress state is denoted as σ_h. This stress state is defined as:

$$\sigma_h = \frac{1}{3}(\sigma_{xp} + \sigma_{yp} + \sigma_{zp}) \quad (2)$$

where:

σ_{xp}, σ_{yp} and σ_{zp} are the principal stresses in the principal directions.

The biaxial crushing stress under the ambient hydrostatic stress state refers to the ultimate compressive strength for the state of biaxial compression superimposed on the hydrostatic stress state, (f_1). The uniaxial crushing stress under the ambient hydrostatic stress state refers to the ultimate compressive strength for a state of uniaxial compression superimposed on the hydrostatic stress state, (f_2). The failure surface can be defined with a minimum of two constants, f_{ct} and f_c. The other three constants (f'_{cb}, f_1, f_2) are defaults to those defined by William and Warnke [6]:

$$f'_{cb}=1.2\ f'_c \quad (3)$$

$$f_1=1.45\ f'_c \quad (4)$$

$$f_2=1.725\ f'_c \quad (5)$$

These stress states are only valid for stress states which satisfy the condition:

$$\sigma_h \le \sqrt{3}\, f'_c \quad (6)$$

Material Model Number (2) refers to the LINK8 bar element. The LINK8 element is being used for prestress tendon and it is assumed to be bilinear isotropic material. For linear part, it is required to define (E_x) which represents the modulus of elasticity of the steel (E_s). The parameter PRXY represents the Poisson's ratio of the steel (ν_c) which is taken as 0.3. The bilinear model is also satisfied by Von Mises failure criterion and requires the yield stress (f_y) as well as the hardening modulus of the steel to be defined. The hardening modulus (tangent modulus) is assumed to be zero.

Pre stressing stress is entered as a value of initial strain by using the formula of Young's modulus:

$$E = \frac{\sigma}{\varepsilon} \quad (7)$$

The value of (E_s) for prestressing bar is assumed to be 1.86×10^5 MPa [9] while the value of initial stress is (5 MPa) as used in experimental study, then the initial strain was calculated and its value was (2.7×10^{-5} mm/mm).

Material Model Number (3 & 4) refers to LINK180 bar element. The LINK180 element is being used for steel reinforcement and it is assumed to be bilinear isotropic

material. For linear part, it is required to define (E_x) which represents the modulus of elasticity of the steel (E_s) and is taken as 1.98 x 10^5 MPa for longitudinal bars and 2.06 x 10^5 MPa for stirrups. The parameter PRXY represents the Poisson's ratio of the steel (ν_c) which is taken as 0.3. The bilinear model is also satisfied by Von Mises failure criterion and requires the yield stress (f_y) as well as the hardening modulus of the steel to be defined. The hardening modulus (tangent modulus) is assumed to be zero.

Material Model Number (5) refers to SHELL41 element which represents the CFRP. The CFRP is assumed to be orthotropic material. (E_x) represents the modulus of elasticity of CFRP (E_{CFRP}) and is taken as 2.3 x 10^5 MPa, PRXY represents the Poisson's ratio of CFRP (ν_{CFRP}) which is taken as 0.3, and ultimate stress (f_t) is considered to be 3400 MPa as in tests.

Material Model Number (6) refers to SHELL41 element which represents the Steel plates. The steel plates are assumed to be linear isotropic material. The modulus of elasticity is assumed to be 2 x 10^5 MPa and Poisson's ratio is 0.3.

2. Modeling & Meshing

The following steps are adapted to model and mesh the tested columns:

Step 1: The concrete is modeled separately as volume with dimensions (200 x 200 x1300) mm.

Step 2: After creating the volume, a finite element analysis requires meshing of the model. The model is divided into a number of small brick elements as shown in Figure (4). In the present study, the concrete volume is divided into 3328 elements with (25, 25, 25) mm.

Step 3: Discrete representation is used to model all types of reinforcement (prestressing bar, longitudinal bars, and ties). No mesh of the reinforcement is needed because individual elements are created in the modeling through the nodes created by the concrete volume. Concrete cover is chosen to be (25 mm) as same as tests. Figure (5) shows reinforcement representation for specimen (Re-1), which is the same as that of specimen (CFS-1) but without using stirrups.

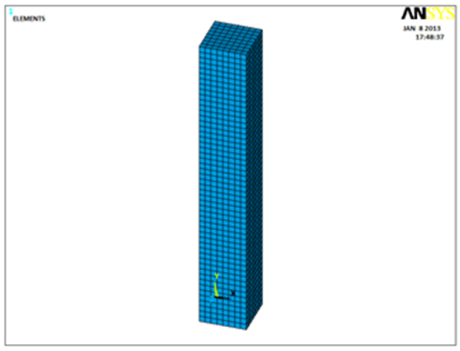

Figure (4). *Mesh of the concrete volume for column specimens Re-1 & CFS-1*

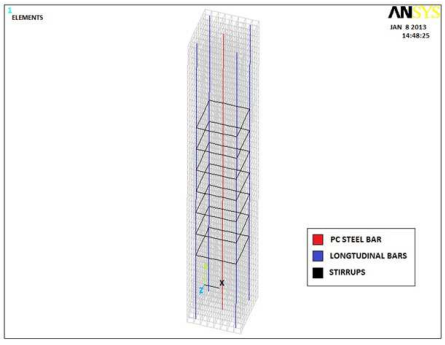

Figure (5). *Reinforcement representation for column specimen Re-1 using LINK8 & LINK180*

Table (5). *Material properties for column specimen Re-1 [5]*

		MATERIAL PROPERTIES	
CONCRETE	E_c	Young's modulus (MPa)*	29501.6
	f_c'	Compressive strength (MPa)	39.4
	f_t	Tensile strength (MPa)	3.24
	ν_c	Poisson's ratio**	0.2
		STRESS-STRAIN RELATIONSHIP OF CONCRETE IN COMPRESSION	
	Point	**Strain**	**Stress**
	1	0.00040	11.82
	2	0.00097	25.24
	3	0.001535	34.05
	4	0.002103	38.30
	5	0.002671	39.4
	6	0.003	39.4
PRESTRESS BAR	E_s	Young's modulus (MPa)	1.86 x 10^5
	f_y	Yield stress (MPa)	410
	ν_e	Poisson's ratio**	0.3
	A	Cross sectional area (mm^2)	283.5
LONGTUDINAL REINF.	E_s	Young's modulus (MPa)	1.98 x 10^5
	f_y	Yield stress (MPa)	356
	ν_e	Poisson's ratio**	0.3
	A	Cross sectional area (mm^2)	132.8

CFRP	**t**	Thickness (mm)	1.33
	E_{CFRP}	Young's modulus (MPa)	2.3 x 10^5
	f_t	Ultimate stress (MPa)	3400
	v_{CFRP}	Poisson's ratio**	0.3
STEEL PLATE	**t**	Thickness (mm)**	2
	E_P	Young's modulus (MPa)**	200000
	v_P	Poisson's ratio**	0.3

* $E_c = 4700\sqrt{f_c'}$ ** Assumed values

Table (6). *Material properties for column specimen CFS-1 [5]*

		MATERIAL PROPERTIES	
CONCRETE	**E_c**	Young's modulus (MPa)*	29501.6
	f_c'	Compressive strength (MPa)	39.4
	f_t	Tensile strength (MPa)	3.24
	v_c	Poisson's ratio**	0.2
		STRESS-STRAIN RELATIONSHIP OF CONCRETE IN COMPRESSION	
	Point	**Strain**	**Stress**
	1	0.00040	11.82
	2	0.00097	25.24
	3	0.001535	34.05
	4	0.002103	38.30
	5	0.002671	39.4
	6	0.003	39.4
PRESTRESS BAR	**E_s**	Young's modulus (MPa)	1.86 x 10^5
	f_y	Yield stress (MPa)	410
	v_e	Poisson's ratio**	0.3
	A	Cross sectional area (mm^2)	283.5
LONGTUDINAL REINF.	**E_s**	Young's modulus (MPa)	1.98 x 10^5
	f_y	Yield stress (MPa)	356
	v_e	Poisson's ratio**	0.3
	A	Cross sectional area (mm^2)	132.8
LATERAL TIES (STIRRUPS)	**E_s**	Young's modulus (MPa)	2.06 x 10^5
	f_y	Yield stress (MPa)	360
	v_e	Poisson's ratio**	0.3
	A	Cross sectional area (mm^2)	78.6
STEEL PLATE	**t**	Thickness (mm)**	2
	E_P	Young's modulus (MPa)**	200000
	v_P	Poisson's ratio**	0.3

* $E_c = 4700\sqrt{f_c'}$ ** Assumed values

Step 4: Representation of CFRP in specimen CFS-1 is shown in Figure (6). These sheets are executed by using the existing nodes of concrete thus no meshing process is required.

Step 5: Steel plates are executed by using the existing nodes of concrete thus no meshing process is required. SHELL41 is also used to represent them. Steel plate's representation is shown in Figure (7).

Step 6: The command merge item merges separated entities that have the same location. These items will then be merged into single entities.

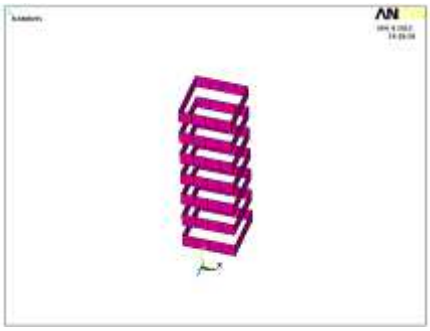

Figure (6). *CFRP representation for column specimen CFS-1 using SHELL41*

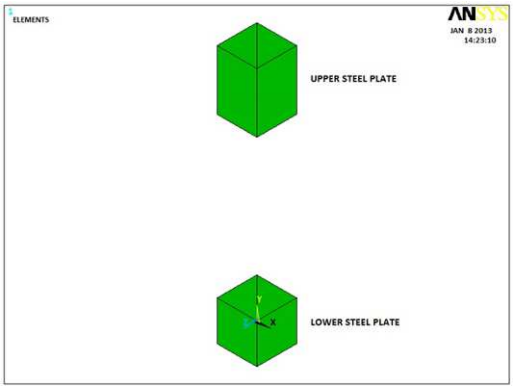

Figure (7). *Steel Plates representation for column specimen Re-1 & CFS-1 using SHELL41*

3. Loading and Boundary Conditions

Displacement boundary conditions are needed to constrain the model to get correct solution. As same as test, the bottom (200 mm) of all specimens was fixed at X, Y, and Z directions in addition to the base of column.

The applied load is performed as couples of forces applied oppositely at the upper (300 mm). A torque of (23.4 kN.m) is applied on column. The small forces for each node were calculated by dividing the primary force by the number of nodes for each side, as shown in Figure (8).

Torsional moment was controlled and loading divided into 180 steps.

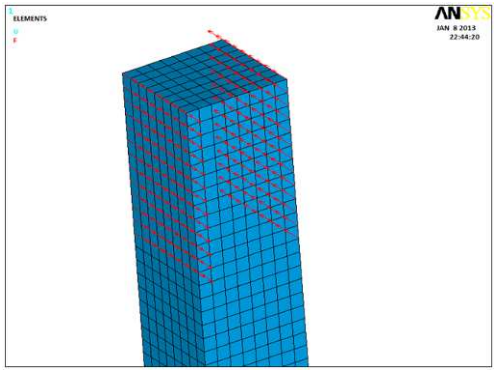

Figure (8). *Torsional loading for column specimens Re-1 & CFS-1*

4. Analysis Results

The finite element analysis of the model is set up to examine the torsional capacity of column specimens, Torque -twist results, distribution of displacements, and cracking conditions. The Newton-Raphson method is used to compute the nonlinear response. The application of the loads up to failure is done incrementally as required by the Newton-Raphson procedure.

4.1. Torque & Angle of Twist

Torque – Twist relations is the most important and significant configuration to study torsional problems. In ANSYS solutions, there is difficulty in obtaining direct results of twisting of concrete members because SOLID65 which is the unique element designed to represent concrete material in ANSYS modeling has only three degrees of freedom solution (U_x, U_y and U_z). There are no results regarding the rotation of nodes in the three directions (ROTX, ROTY, and ROTZ).

So it is necessary to suppose a method for obtaining angles of twist using the displacement results obtained by ANSYS.

The method of measuring angles of twist in experimental research used for verification is adopted to get angle of twist for each loading step with some modifications. The Aluminum bars used in experimental study with length of (800 mm) was neglected.

Displacements in x – direction of end points for upper bar (AB) and lower bar (CD) is used to calculate the angle of twist as shown in Figure (9)

The formula is modified as following:

$$\theta = \frac{\frac{V_1 - V_2}{800} - \frac{V_3 - V_4}{800}}{500} \quad \text{rad/mm} \qquad \dots (8)$$ Experimental Formula

$$\theta = \frac{\frac{Ux_{96} - Ux_{521}}{200} - \frac{Ux_{76} - Ux_{501}}{200}}{500} \quad \text{rad/mm} \qquad \dots (9)$$ Present Study Formula

Where:

θ: Angle of Twist (rad/mm)

Ux_{96}: Displacement in x-direction of point A

Ux_{521}: Displacement in x-direction of point B

Ux_{76}: Displacement in x-direction of point C

Ux_{501}: Displacement in x-direction of point D

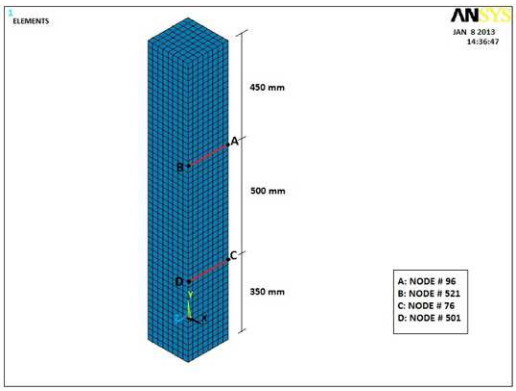

Figure (9). *Locations of bars nodes used to calculate angles of twist*

The deformed shapes that show the displacements variation in x, y, and z directions and vector summation of displacements for Re-1 specimen are shown in Figures (10). Displacements results which are the basics of twist results can be described as follows:

1. Regarding each direction, the variation of displacements was arranged to form layers, each layer represent a range of values for displacement as shown in Figure (11).
2. The values for summation of displacements are increased as the nodes locations are away from the center of the column forming circular layers as shown in

Figure (12) reaching its maximum values near corners. Generally, it is obvious that the values are increased as the nodes are away from the fixed ended base.

3. In x & z directions, the values of displacements for nodes at each edge are opposite in direction with these at the facing edge in the same section due to torsional effect.

The displacement results of analysis performed using finite element code ANSYS, version 14, have been used to calculate angle of twist for each load step and then compared with Torque – angle of twist curves obtained from experimental work.

Regarding specimen Re-1, the ultimate load has been obtained once the analysis has been stopped simply due to lack of convergence. The numerical ultimate load is (12.7 kN.m) (0.00574 rad/m), while the experimental ultimate load is (11.8 kN.m) (0.00574 rad/m). The ratio of the predicted ultimate load to the experimental value is (7.6 %). Plotting the ANSYS curve against the experiment work in Figure (13), which is shows a reasonable agreement.

About specimen CFS-1, the same procedure was done and the ultimate load was (15.43 kN.m) (0.0066 rad/m) compared with the value of experimental work which is (14.13 kN.m) (0.00675 rad/m). The ratio of the predicted ultimate load to the experimental value is (9.2 %). Figure (14) shows the two curves with very good agreement.

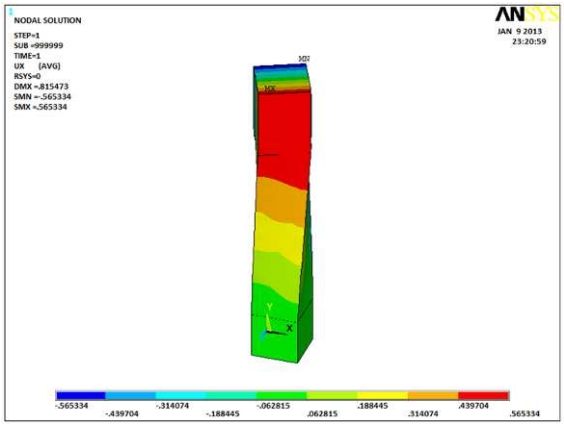

Figure (10). *Variation of displacements in X – direction for specimen Re-1*

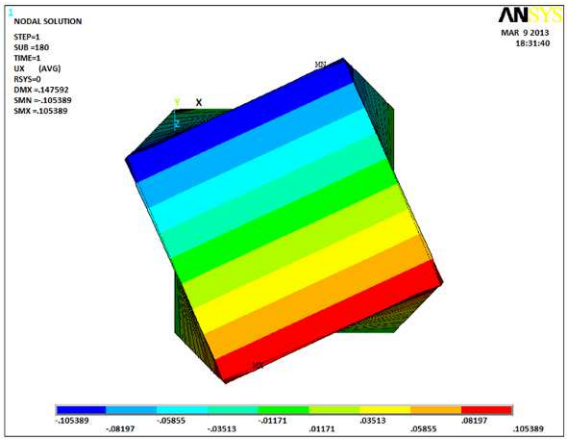

Figure (11). *Distribution of displacements in X – direction in form of layers*

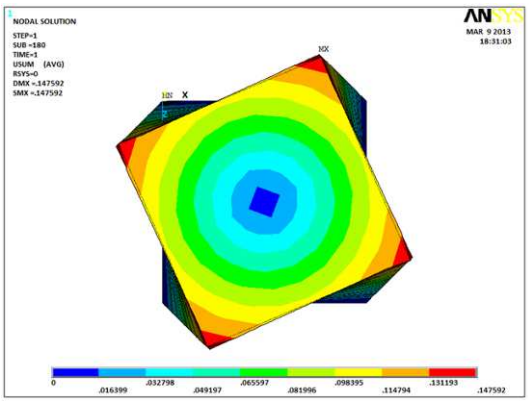

Figure (12). *Distribution of vector summation of displacements in circular layers*

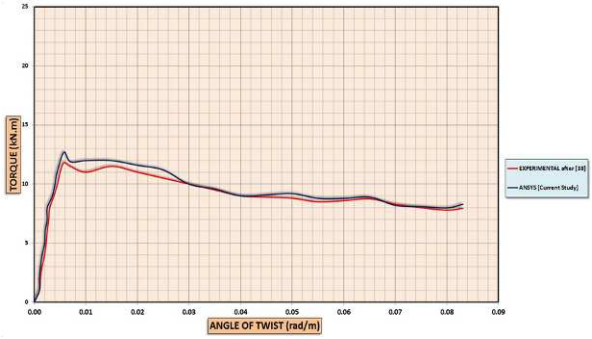

Figure (13). *Experimental & ANSYS Torque – Twist curves for column specimen Re-1*

Figure (14). *Experimental & ANSYS Torque – Twist curves for column specimen CFS-1*

4.2. Cracks Conditions

The crack/crushing patterns in the column can be obtained using the Crack/Crushing plot option in finite element code ANSYS, version 14. Vector Mode (wireframe) plots must be turned on to view the crack/crushing in the model. In the non-linear region of the response, subsequent cracking occurs as more loads are applied to the column. First cracking started occurring at torsional moment 10.9 kN.m, as shown in Figure (15); the location of the first cracking is nearly the lower fixed end at about 220 mm from bottom of column.

Once the steel reinforcement starts to yield, the displacements of the column begin to increase at a higher rate as more load increments are applied. The ability of the column to distribute load throughout the cross-section has

diminished greatly. Therefore, greater deformation occurs at the column corners. The cracking patterns in the integration points, the final cracks are shown in Figure (16).

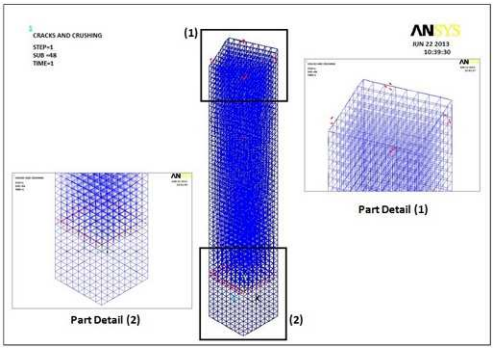

Figure (15). *First Crack Pattern for column specimen CFS-1*

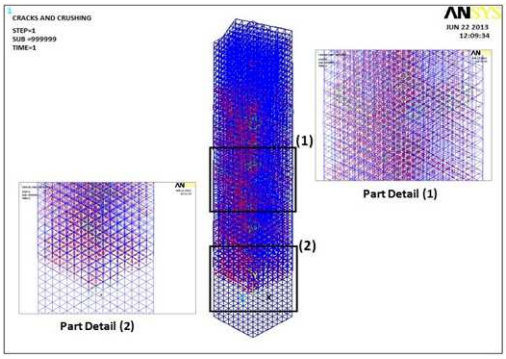

Figure (16). *Final Cracks Pattern for column specimen CFS-1*

5. Parametric Study

In order to investigate the effects of most important parameters affecting the torsional capacity of RC columns strengthened with CFRP, a parametric study have been carried out in this chapter, these parameters include:

1 Presence (Distribution) of CFRP
2 Effect of CFRP Thickness
3 Effect of Interface Type between CFRP Layer and Concrete Surface
4 Effect of CFRP Orientation (Zebra Shape)
5 Effect of Applying Axial Load in addition to Torque

In each numerical test, all properties of the system will be held constant except the specified parameter which is considered to change to show the effects of the considered parameter on the behavior of column and to isolate the effects of other parameters.

Experimental column specimen designated as [CFS-1] that analyzed in the previous chapter are further reinforced with stirrups as same method of reinforcing used in specimen [Re-1], the prestressing tendon is neglected and the resulted column have been chosen as a numerical reference case and designated as [REF-1] to represent the real case of most RC columns strengthened with CFRP in several structural buildings and to compare its torsional capacity with other numerical tests carrying out a parametric study.

5.1. Presence of CFRP

In this sub-section, the effects of distribution of CFRP on the response of concrete column is investigated, two types of CFRP distribution are presented as follows:

1. TYPE I: Strip width = 50 mm with 50 mm spaces between them [REF-1].
2. TYPE II: Strip width = 100 mm with 50 mm spaces between them [C1-1].

Figure (17) shows the two types of CFRP distribution.

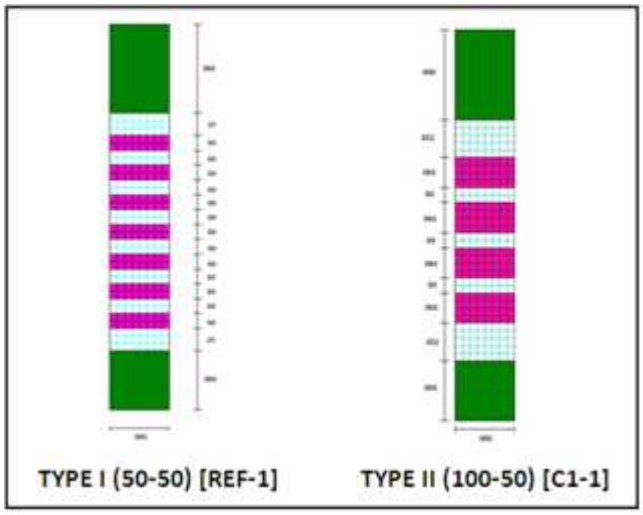

Figure (17). *Distribution types of CFRP*

The results showed that the torsional capacity increased by 5.84 % when using stirrups in reinforcing column [REF-1] in comparison with numerical value of torsion in specimen [CFS-1] and 3.95 % when using type II of distribution (100-50) in specimen [C1-1], this is due to the increase in total area of CFRP. Figure (18) shows the effect of presence of CFRP on torque - twist behavior.

Figure (18). *Effect of presence of CFRP on torque - twist behavior*

5.2. Effect of CFRP Number of Layers (CFRP Thickness)

In this sub-section the effects of CFRP layers total thickness on the torsional capacity of concrete column strengthened with CFRP is investigated. To conduct this

study, three types of columns are used with different numbers of layers, the columns analyzed are:

1. [REF-1] [4 layers of CFRP / 1.33 mm with stirrups in reinforcement].
2. [C2-1] [2 Layers of CFRP / 0.66 mm].
3. [C2-2] [8 Layers of CFRP / 2.66 mm].

The results showed that the torsional capacity increased by 1.88 % when doubling the thickness of CFRP layers to be 2.66 mm while the torsional capacity decreased by 2.92 % when decreasing the thickness of layers to the half to be 0.655 mm in comparison with the value of [REF-1]. Figure (19) represent the Effect of CFRP thickness on torque - twist behavior.

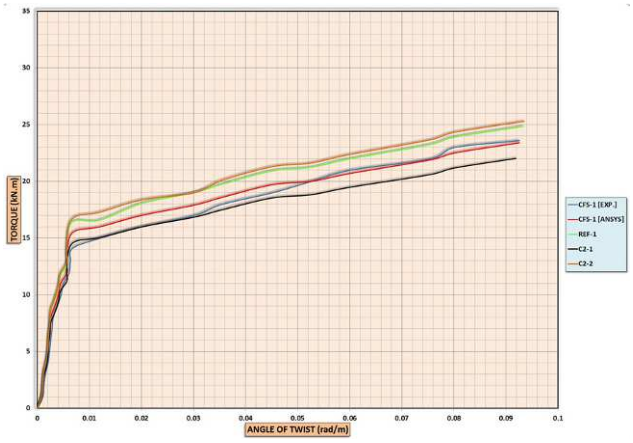

Figure (19). *Effect of CFRP thickness on torque - twist behavior*

5.3. Effect of Interface Type between CFRP Layer and Concrete Surface

In this sub-section the effect of full and partial contact between CFRP and concrete surface on the response of concrete columns is investigated. For the above purpose, two types of columns strengthening are considered. The first column specimen is [REF-1] and the second is [C1-1] described previously in section 5.2, the two columns are analyzed for both cases of interface described as follows:

1. Column specimens [REF-1] & [C1-1] [Full contact generated from concrete nodes]
2. Column specimens [C3-1] & [C3-2] [Interface elements with TAUMAX equal to 4 MPa) [5]
3. Column specimens [C3-1] & [C3-2] denoted for partial interface for Type I and Type II of CFRP distribution respectively.

The results showed decreasing in torsional capacity when using partial interface instead of full interface, the decreasing was 1.79 % for type I and 1.6 % for type II. These results are reasonable because full bond interface make column specimens stiffer and this need a greater value of torque to reach failure stage. Figure (20) display the effect of interface type between CFRP & concrete on torque - twist behavior.

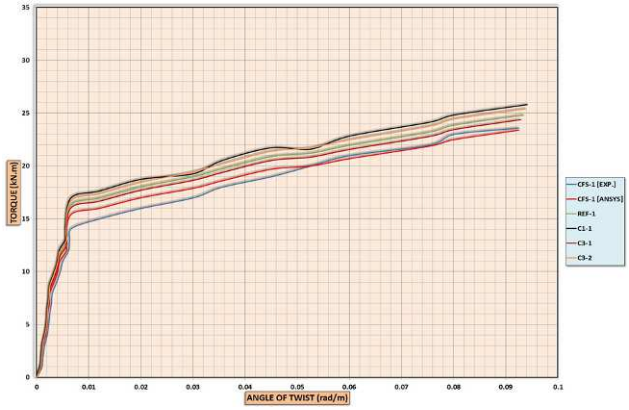

Figure (20). *Effect of interface type between CFRP & concrete on torque - twist behavior*

5.4. Effect of CFRP Orientation (Zebra Shape)

The orientation of CFRP is another important factor affecting the torsional capacity of RC columns. Since the inspections on typical concrete columns and the experimental works done on columns subjected to torque showed that the cracks are appeared in an oblique direction, the CFRP here are fixed in an opposite direction of the predicted cracks to investigate its effects on increasing the torsional capacity of columns. In this subsection, three types are presented:

1. STRAIGHT: The strips are fixed in straight horizontal direction and fibers oriented horizontally as described previously in section (5.2).
2. INCLINED 45^{o}: The strips are fixed in inclined direction with angle of 45^{o} opposite to the direction of torsional cracks as shown in Figure (21).
3. ZEBRA SHAPE: The strips are fixed in straight direction but its fibers are oriented obliquely with angle of 45^{o} opposite to torsional cracks direction.

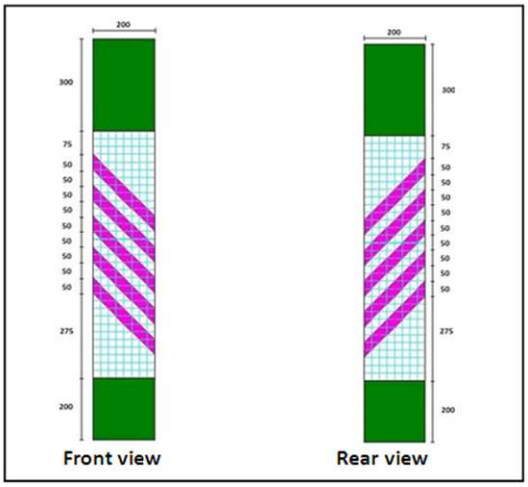

Figure (21). *Inclined type of fixing CFRP with angle 45^{o} [INCLINED 45^{o}]*

For each type of orientation, the results are shown for both full and partial interface between CFRP and concrete to display the combined effects. Columns [REF-1], [C4-1], and

[C4-2] represented the full interface for the three types of orientation respectively, while columns [C3-1], [C4-3], and [C4-4] represented the partial interface. Finally, another case denoted as [C4-5] with zebra shaped fibers and (8) layers is investigated.

The results showed that zebra shape is the best way to increase the torsional capacity of RC columns with increasing of torsional capacity by 16.85 % while inclined type of orientation increased the torsional capacity 7.91 % comparing with the straight type of orientation which represented in column [REF-1] . Same method is done for partial interface and the ratios are generally decreased to be 15.63 % and 5.74 % respectively. Regarding column specimen [C4-5], the gain of torsional capacity was 21.09 % which is the greatest value among all. Figure (22) represent the effect of CFRP orientation on torque - twist behavior.

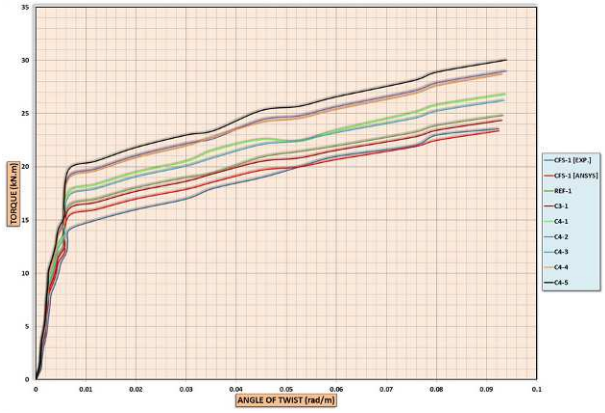

Figure (22). *Effect of CFRP orientation on torque - twist behavior*

5.5. Effect of Applying Axial Load in Addition to Torque

Since the real cases of most structural columns are columns subjected to axial loads, therefore the effect of applying axial load in addition to torque is investigated in this sub-section of parametric study.

In addition to the control specimen [REF-1] which is not subjected to axial loads, four specimens are analyzed described as following:

1. [C5-1][Axial load of 81 kN-CFRP TYPE I (50-50)].
2. [C5-2][Axial load of 162 kN-CFRP TYPE I (50-50)].
3. [C5-3][Axial load of 81 kN]-CFRP TYPE I (100-50)].
4. [C5-4][Axial load of 162 kN]-CFRP TYPE I (100-50)].

The results showed increasing in torsional capacity by 6.31 % when applying a load of (81 kN) and 11.39 % when doubling the load to be (162 kN) regarding specimens with type I distribution, and the results for type II distribution were 9.32 % and 13.37 % respectively . Figure (23) shows the Effect of applying axial load on torque - twist behavior.

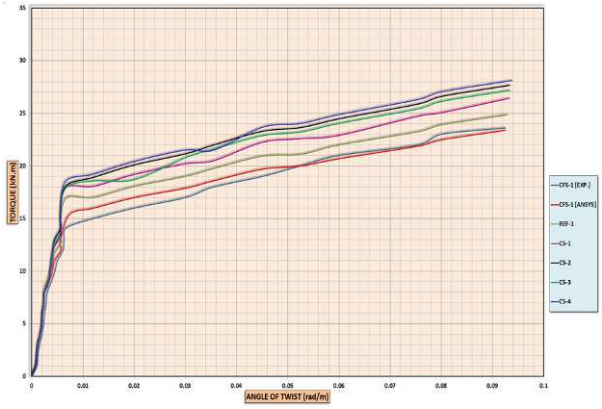

Figure (23). *Effect of applying axial load on torque - twist behavior*

Figure (24) show the overall graph representing the torque twit curves of all column specimens used in parametric study, it is clear that column [C4-5] shows the torsional behavior of combined effects of all parameters. A summary for columns specimens used in parametric study with full description of each one and the percentages of torsional capacity was presented in Table (7).

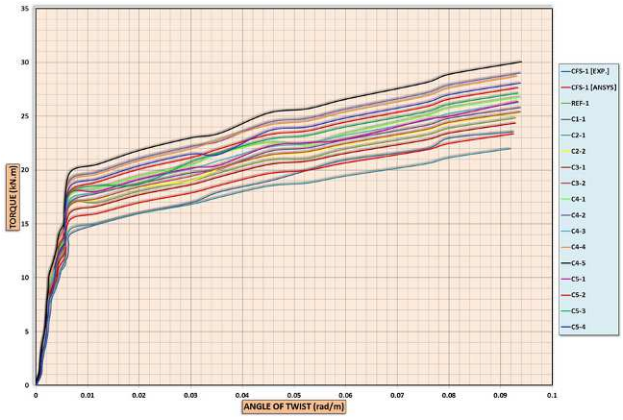

Figure (24). *Overall torque – twist behavior for cases used in parametric study*

Table (7). *Summary of Cases investigated in Parametric Study*

CASES	PRESENCE OF CFRP	CFRP THICKNESS	TYPE OF INTERFACE	CFRP ORIENTATION	AXIAL LOAD	PERCENTAGE OF TORSIONAL CAPACITY
REF-1	TYPE I (50-50)	1.33 mm (4 LAYERS)	FULL	STRAIGHT	NO AXIAL LOAD	0.0 % [REFERENCE VALUE]
C1-1	TYPE II (100-50)	1.33 mm (4 LAYERS)	FULL	STRAIGHT	NO AXIAL LOAD	+3.95 %
C2-1	TYPE I (50-50)	0.665 mm (2 LAYERS)	FULL	STRAIGHT	NO AXIAL LOAD	-2.92 %
C2-2	TYPE I (50-50)	2.66 mm (8 LAYERS)	FULL	STRAIGHT	NO AXIAL LOAD	+1.88 %

CASES	PRESENCE OF CFRP	CFRP THICKNESS	TYPE OF INTERFACE	CFRP ORIENTATION	AXIAL LOAD	PERCENTAGE OF TORSIONAL CAPACITY
C3-1	TYPE I (50-50)	1.33 mm (4 LAYERS)	PARTIAL	STRAIGHT	NO AXIAL LOAD	-1.79 %
C3-2	TYPE II (100-50)	1.33 mm (4 LAYERS)	PARTIAL	STRAIGHT	NO AXIAL LOAD	+2.35 %
C4-1	TYPE I (50-50)	1.33 mm (4 LAYERS)	FULL	*INCLINED 45°	NO AXIAL LOAD	+7.91 %
C4-2	TYPE I (50-50)	1.33 mm (4 LAYERS)	FULL	**ZEBRA	NO AXIAL LOAD	+16.85 %
C4-3	TYPE I (50-50)	1.33 mm (4 LAYERS)	PARTIAL	*INCLINED 45°	NO AXIAL LOAD	+5.74 %
C4-4	TYPE I (50-50)	1.33 mm (4 LAYERS)	PARTIAL	**ZEBRA	NO AXIAL LOAD	+15.63 %
C4-5	TYPE I (50-50)	2.66 mm (8 LAYERS)	FULL	**ZEBRA	NO AXIAL LOAD	+21.09 %
C5-1	TYPE I (50-50)	1.33 mm (4 LAYERS)	FULL	STRAIGHT	AXIAL LOAD (81 kN)	+6.31 %
C5-2	TYPE I (50-50)	1.33 mm (4 LAYERS)	FULL	STRAIGHT	AXIAL LOAD (162 kN)	+11.39 %
C5-3	TYPE II (100-50)	1.33 mm (4 LAYERS)	FULL	STRAIGHT	AXIAL LOAD (81 kN)	+9.32 %
C5-4	TYPE II (100-50)	1.33 mm (4 LAYERS)	FULL	STRAIGHT	AXIAL LOAD (162 kN)	+13.37 %

NOTES: (1) Column specimen CFS-1[ANSYS] is free of stirrups; other cases are reinforced with stirrups.
(2) *INCLINED 45°: Strips inclined with 45° ** ZEBRA: Horizontal strips with inclined fibers

6. Conclusions

1 Generally, the proposed F.E procedure used for predicting the torsional behavior of square RC columns strengthened with CFRP proved its efficiency in analysis of such types of columns. The results showed acceptable agreement of experimental works used for verification. The maximum difference was 7.6 % for columns specimen [Re-1] reinforced with stirrups without CFRP, and 9.2 % for column specimen [CFS-1] strengthened with CFRP. Such results can be considered reasonable results since experimental tests reflect reality while the F.E.A is a numerical technique with stiffer behavior.

2 For all columns subjected to torque, the distribution of each direction of nodal displacements showed that it is arranged in form of layers. Each layer represents a range of values for displacements. The vector summation of displacements is increased as the nodes locations are away from the center of column, forming circular layers and reaching its maximum values at corners of column faces. On the other hand, the angles of twist are increased as the nodes are away from the fixed ended base due to torsional effect on column.

3 The ultimate torsional capacity is increased with 3.95 % as the area of CFRP used in strengthening columns is increased from 4 sheets of 100 mm width and spaces of 50 mm to 7 sheets of 50 mm width and spaces of 50 mm too.

4 The torsional capacity is not affected significantly by the value of CFRP thickness; it is increased by 1.88 % when doubling the thickness of CFRP from 1.33 mm to 2.66 mm, while it is decreased by 2.92 % when decreasing the thickness of layers to the half to be 0.655 mm in comparison with the value of reference specimen.

5 There was a general decreasing in torsional capacity when using partial interface instead of full interface. The decreasing was 1.79 % for columns strengthened with CFRP type I (50-50 mm) and 1.6 % for those strengthened with type II (100-50 mm). These results are reasonable because full bond interface make column specimens stiffer and this need a greater value of torque to reach failure stage.

6 The most important factor affecting significantly the torsional capacity of columns strengthened with CFRP is the orientation of CFRP fibers. The results of analysis showed that zebra shape (where fibers are perpendicular to cracks direction) is the best way to increase the torsional capacity of RC columns with increasing of torsional capacity by 16.85 % for specimen with (4 layers) and 21.09 % for specimen with (8 layers), while inclined type of orientation (where sheets are fixed obliquely with 45o and straight fibers) increased the torsional capacity by 7.91 % comparing with the straight type of orientation which represented in reference column (with straight orientation for sheets and their fibers).

7 Axial loads are subjected to the columns under investigation in addition to torque to represent real loading case of concrete columns and the results showed general increasing in torsional capacity by 6.31 % when applying a load of (P=81 kN) (τ/P = 0.289 kN.m/kN) and 11.39 % when doubling the load to be (P=162 kN) (τ/P = 0.143 kN.m/kN) regarding specimens with (Type I) distribution, and the results for (Type II) distribution were 9.32 % and 13.37 % respectively. All for the same cross sectional area.

References

[1] Shrive P.L., Azarnejad A., Tadros G., McWhinnie C., and Shrive N.G., "Strengthening of concrete columns with carbon fiber reinforced polymer wrap ", Canadian Journal of Civil Engineering, May, Vol. 30, 2003, pp. 543–554.

[2] Norayanan R., "Axially Compressed Structures Stability and Strength", Applied Science Publishers, LTD., 1982.

[3] Zhou J., Hirosawa M., Kondo T., and Shimizu Y., "Effect of the torsional moment on the shear strength of reinforced concrete columns due to eccentric jointing of beam to column ", 12th world conference of earthquake engineering, Auckland, New Zealand, Sunday, 2000.

[4] Manopulo N., "An Introduction to Finite Element Methods" Seminar: Interplay of Mathematical Modeling and Numerical Simulation, May, 2005, 16pp.

[5] He, H.M., and Kiyomiya, O., "Study on torsion properties of carbon fiber sheets strengthened PC member with zebra-shaped", Journal of Structural Eng./ Earthquake Eng., JSCE, Vol. 25, No 1, 2008, pp. 1s-15s.

[6] ANSYS, "ANSYS Help", Release 14.0, Copyright 2013.

[7] ACI Committee 318, "Building Code Requirements fo Structural Concrete (ACI 318M-11) and Commentary (ACI 318R-11)", American Concrete Institute, Farmington Hills, MI, 2008, 466 pp.

[8] Kachlakev D., Miller Th., Yim S., Chansawat K. and Potisuk T., "Finite Element Modeling of Reinforced Concrete Structures Strengthened with FRP Laminates", Report for Oregon Department Of Transportation, May, 2001, 99 pp.

[9] Nilson A., Darwin D., Dolan C., “Design of Prestressed Concrete”, John Wiley & sons, 2nd edition, 1987, 43 pp.